

Characteristics of tropical cyclone activity over the South China Sea: Local and nonlocal tropical cyclones

Liang Wu^{1,*}, Hongjie Zhang¹, Jau-Ming Chen², and Tao Feng³

¹Center for Monsoon System Research, Institute of Atmospheric Physics, Chinese Academy of Sciences, Beijing
²Department of Maritime Information and Technology, National Kaohsiung University of Science and Technology, Kaohsiung
³College of Oceanography, Hohai University, Nanjing

Article history:

Received 30 March 2019

Revised 13 June 2019

Accepted 1 July 2019

Keywords:

Local and nonlocal Tropical Cyclones, South China Sea (SCS), Climatological characteristic, Interdecadal variability

Citation:

Wu, L., H. Zhang, J.-M. Chen, and T. Feng, 2020: Characteristics of tropical cyclone activity over the South China Sea: Local and nonlocal tropical cyclones. *Terr. Atmos. Ocean. Sci.*, 31, 261-271, doi: 10.3319/TAO.2019.07.01.02

ABSTRACT

The South China Sea (SCS) is affected by two types of tropical cyclones (TCs): those locally formed in the SCS (local TCs) and those traversing the SCS (nonlocal TCs). In this study, the characteristics of these two types of SCS TCs are investigated for the period of 1979 - 2016. It is shown that only 2.3 per year (10.9%) form in the SCS (local TCs) and 5.5 per year (25.5%) pass from the western North Pacific (WNP) into the SCS (nonlocal TCs). Nonlocal TCs tend to form in the WNP west of 160°E and cross the Philippines into the SCS with typical straight westward tracks. Local TCs mostly move northwestward or northeastward, and they have shorter tracks, are less intense, and have shorter lifetime compared to nonlocal TCs. Annual TC rainfall in the SCS is primarily attributed to nonlocal TCs, but the slower motion of local TCs (with weaker intensity) increases TC rain-rate and intensity of extreme rainfall. Their genesis locations (tracks) migrate with large-scale environments (steering flows) associated with variations of the monsoon trough and the subtropical high in the WNP. Furthermore, the annual numbers of local and nonlocal TCs exhibit a significant inverse relationship on both interannual and interdecadal timescales; this is especially evident on interdecadal timescales. This interdecadal relationship may be explained by the interdecadal variability of sea surface temperature (SST) in the central Pacific, which drives the changes in the low-level westerlies and the monsoon trough.

1. INTRODUCTION

Tropical cyclones (TCs) affect nearly all coastal areas and are the most important natural disasters in the western North Pacific (WNP). The South China Sea (SCS), a sub-region of the WNP, is a semi-enclosed marginal sea in the western part of the WNP. It has long been recognized that TC activity in the SCS region has different characteristics than that in the other regions of the WNP. There are two kinds of TCs in the SCS: those locally formed in the SCS (local TCs) and those traversing the SCS (nonlocal TCs).

Most local TCs are less intense and are harder to predict than nonlocal TCs, as they have a relatively short time to develop before making landfall. Many studies have focused on the intraseasonal (Ling et al. 2016), interannual (Zuki and Lupo 2008), and interdecadal (Goh and Chan

2009) variations of local TC activity in the SCS. The results indicate that the variability of local TCs might be strongly modulated by several weather and climate systems, such as the Madden-Julian Oscillation (MJO), quasi-biweekly oscillation (QBWO), El Niño-Southern Oscillation (ENSO), and Pacific Decadal Oscillation (PDO). However, there are fewer studies that focus on nonlocal TCs. Chen et al. (2017) shows that nonlocal TCs in the SCS tend to form in the WNP west of 150°E and migrate seasonally with the monsoon trough.

Previous studies on TC activity have found that their behavior is dependent on the large-scale environment. Gray (1968, 1975) indicated that the formation and development of TCs are closely related to large-scale thermodynamic and dynamic conditions. In past decades, examined variables have included sea surface temperature (SST), OLR, relative humidity in the middle troposphere, vertical wind

* Corresponding author
E-mail: wul@mail.iap.ac.cn

shear, upper-level divergence, low-level vorticity and so on (e.g., Briegel and Frank 1997; Chu 2002; Chan and Liu 2004; Cheung 2004; Sobel and Camargo 2005; Wu and Chu 2007; Ramsay et al. 2008; Wu et al. 2012). Movement of TCs is controlled by large-scale steering flows (Holland 1983; Wu and Zhao 2012) and formation locations (Wu and Wang 2004; Wu et al. 2012). Thus, anything affecting these conditions would cause variation in the TC activity. It is well-known that ENSO and PDO play critical roles in the variability of the genesis and tracks of TCs in the WNP and SCS by modulating large-scale oceanic and atmospheric environmental conditions. These processes may be attributed to changes in local large-scale monsoon circulations over the WNP and SCS, such as the monsoon trough (Wu et al. 2012) and subtropical high (Wang et al. 2013).

The present study attempts to characterize local and nonlocal TC activity and background states in the SCS. The objective is to advance our understanding of the impact of TC activity on the SCS and its rim countries. In this paper, section 2 describes data sources and processing methods; section 3 contrasts characteristics of local and nonlocal TCs in the SCS and their corresponding environmental conditions; section 4 gives the relationship between local and nonlocal TCs on an interdecadal timescale and offers a possible interpretation; and section 5 presents a summary of our findings.

2. DATA AND METHODS

The analyses in this study use different datasets extending from 1979 to 2016 and only data from June to November is considered, as these months represent the main TC season in the WNP. The SCS domain is defined as 108 - 120°E, 5 - 22°N, as presented in Fig. 1a. The best-track dataset is from the IBTrACS website archive, and was provided by the Joint Typhoon Warning Center (JTWC) for the period of 1979 - 2016. These data contain the 6-hourly positions and intensities of each TC. JTWC uses 1-min mean wind speed at 10-m height for the maximum sustained wind estimate. In this study, the TCs only include two intensity ranges, tropical storms (lifetime maximum wind speed $> 17 \text{ m s}^{-1}$) and typhoons (categories 1 - 5, lifetime maximum wind speed $> 33 \text{ m s}^{-1}$), as based on the Saffir-Simpson scale (Simpson and Riehl 1981). The time and position of TC genesis is defined as the first time and position when the TC appears on track records.

The atmospheric field data are obtained from the Japanese 55-year Reanalysis (JRA-55) dataset (Kobayashi et al. 2015) and SST field data are from the Hadley Center (Rayner et al. 2003). In addition, the gridded 6-hour accumulation rainfall data are from Climate Forecast System Reanalysis (CFSR) data from NCEP (Saha et al. 2010), and rainfall occurring within a 10° radius (1110 km) around the TC center is identified as TC rainfall. The choice of a 10° (1110-km) radius accounts for the TC rainfall, including the inner core

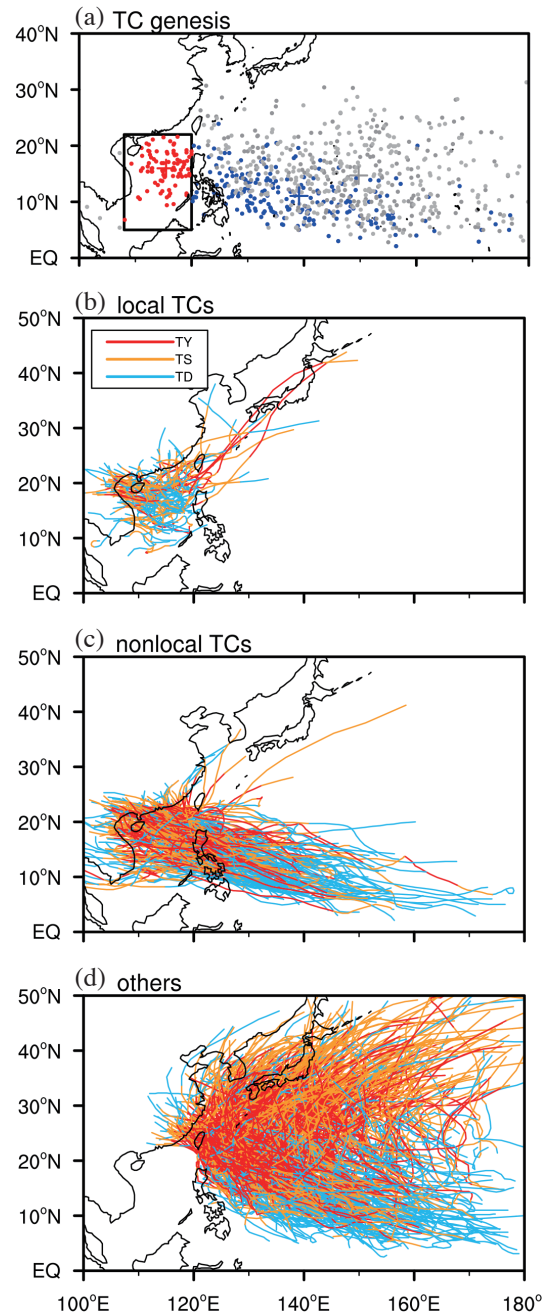


Fig. 1. (a) The formation locations for TC with formation (local TCs, red dots), with passage (nonlocal TCs, blue dots), and without passage (others, gray dots) into the South China Sea (SCS). The South China Sea analysis domain indicated by a rectangular box. The tracks for (b) local TCs, (c) nonlocal TCs, (d) others.

and the adjacent rainbands, which is consistent with other studies (e.g., Kubota and Wang 2009; Bagtasa 2017). Outgoing longwave radiation (OLR) data comes from National Oceanic and Atmospheric Administration (NOAA) polar-orbiting satellites (Liebmann and Smith 1996).

In addition, El Niño, La Niña, and El Niño Modoki years are defined using the values of the Niño-3 and El Niño Modoki indices (EMI, Ashok et al. 2007). The statistical significance of anomalies is estimated using Student's *t* test.

3. CHARACTERISTICS OF LOCAL AND NONLOCAL TC ACTIVITY IN THE SCS

3.1 Genesis and Tracks of TCs

Figure 1a shows the genesis positions of all WNP TCs from 1979 to 2016. During the TC season, the climatological mean number of TCs per year is approximately 21.5 (Fig. 2a). Around one-third of these (7.8 per year) can directly affect the basin of the SCS. However, only 2.3 per year (10.9%) form in the SCS (local TCs), which is similar in area to the other genesis basins of the WNP, and 5.5 per year (25.5%) pass from the WNP into the SCS (nonlocal TCs). The nonlocal TCs tend to form in the WNP west of 160°E, and the mean genesis position, near 11.1°N, 139.1°E, is approximately 11° westward in longitude and 4° southward in latitude away from the position of TCs that do not track into the SCS (Fig. 1a). The local TCs mostly move northwestward or northeastward (Fig. 1b) and have shorter tracks; thus, they are often limited to the SCS. Nonlocal TCs have typical straight west-northwest tracks and cross the Philippines into the SCS (Fig. 1c). The other WNP TCs more frequently take a recurved track, and most of the other TC activity occurs east of the Philippines (Fig. 1d).

Previous studies have demonstrated that the genesis locations and tracks of TCs are closely associated with large-scale circulation changes. To avoid TC signals themselves, composite charts of different kinds of large-scale circulation changes are made using data from 1 day prior to the genesis. Figure 3 shows composite charts of 850-hPa winds, 500-hPa geopotential heights, and TC genesis locations for local, nonlocal, and other TCs. For local TC genesis, anomalous monsoonal westerlies in the tropical WNP and a weaker subtropical high result in a poleward extension in the location of the monsoon trough (Figs. 3a, d). This broad monsoon trough is followed by an enhanced monsoon gyre over the northern SCS. Strong upper-level divergence in the vicinity of low-level cyclonic vorticity drives increased middle relative humidity and deep convection (Fig. 4a), which favor TC genesis in the SCS. The corresponding large-scale steering flow, which is defined as the mean flow from 850 to 300-hPa, shows anomalous cyclonic flow in the northern SCS (Figs. 5a, d). The northwestward (northeastward) motion of local TCs can be attributed to anomalous westerlies (easterlies) as part of this anomalous cyclonic

circulation. Previous studies (Yang et al. 2015; Ling et al. 2016) have noted that this change in the steering flow shows an obvious intraseasonality in response to intraseasonal oscillations (ISOs) in the northern SCS. The numbers of local and nonlocal TCs differ in seasonal cycles (Fig. 2). Local TCs are more active in August and September, but nonlocal TCs are more active in October, November, and July (Fig. 2a). It is noted that the percentage of local TCs in May is larger compared to that in other months due to the TC season starting earlier in the SCS (Fig. 2b). The seasonal variability of local and nonlocal TCs is primarily modulated by Asian monsoon systems such as the monsoon trough and the subtropical high (Chen et al. 2017).

For nonlocal TC genesis, a westward extension of the enhanced subtropical high strengthens anomalous easterlies between 10 and 20°N along the southern edge of the subtropical high, leading to a southward shifting of anomalous westerlies. These anomalies drive a narrow monsoon trough to shift southeastward and extend through the western part of the WNP. Increased low-level cyclonic vorticity and upper-level divergence, 500 - 700-hPa relative humidity, and deep convection center shifts to the western part of the tropical WNP (Fig. 4b) accompanying this monsoon trough development, indicating potential increases of TC genesis in the region. The corresponding large-scale steering flow shows that significant anomalous easterlies extend from the WNP to the SCS between 10 and 20°N (Figs. 5b, e), leading to a typical westward track of TCs from the WNP through the Philippines and into the SCS.

For other TC genesis, following the slightly northward-shifted subtropical high, enhanced anomalous westerlies extend poleward to higher latitudes (20°N). The enhanced monsoon trough is shifted slightly eastward and northward with respect to nonlocal TCs. This generates a northeastward shift in anomalous cyclonic vorticity, upper-level divergence, relative humidity, and convection (Fig. 4c), and thus leads to eastward and northward shifts in the positions of other TC genesis. Following the northeastward shift of the subtropical high, the anomalous steering flows easterlies shift to north of 20°N (Figs. 5b, e), producing the recurved steering flows from northwestward to northeastward around 25°N. As a result, TC tracks trend to move northwestward or to recurve from northwestward to northeastward around the east of the Philippines without passage into the SCS.

3.2 Intensity and Rainfall of TCs

Figure 6a shows the population versus intensity (maximum wind speeds) of local and nonlocal TCs in the SCS. There is a notable difference between the frequencies of intense local and nonlocal TCs: the majority of local TCs have rather weak intensities (more tropical storms), while nonlocal TCs are more likely to develop into intense storms and typhoons. This could be due to the longer storm lifespan of

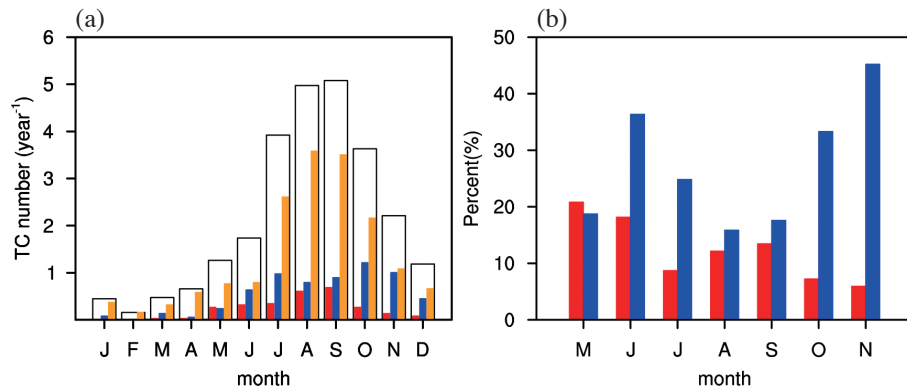


Fig. 2. (a) Histograms of monthly genesis frequency of TCs over the WNP (open bar) from 1965 to 2016. The shaded bars represent monthly genesis frequency of local (red) and nonlocal (blue) TCs over the SCS, and other TCs over the WNP (orange). (b) The ratio of local (red) and nonlocal (blue) TCs in the SCS to total TCs in the WNP for the months of June to November.

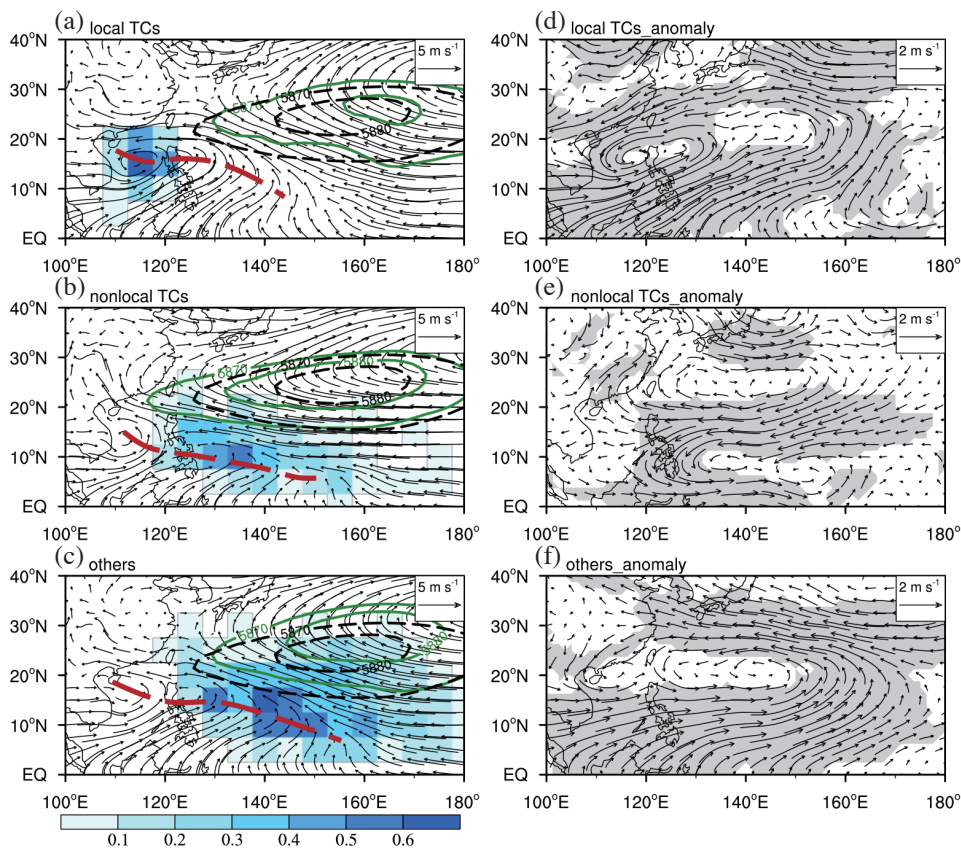


Fig. 3. The composite total TC genesis (in a $5^\circ \times 5^\circ$ box, shaded), 850-hPa wind (m s^{-1} ; vector), and 500-hPa geopotential height (gpm, dashed black lines) for average of 1 day prior to the genesis of (a) local TCs, (b) nonlocal TCs, and (c) other TCs in the SCS during June to November. (d) - (f) as (a) - (c), but for 850-hPa wind anomalies (m s^{-1} ; vector). The shadings denote regions of anomalies significant at 95% confidence level. The monsoon trough (MT) is denoted by a red, thick-dashed line. Solid green lines indicate the climatological mean 500-hPa geopotential height (gpm) during June to November.

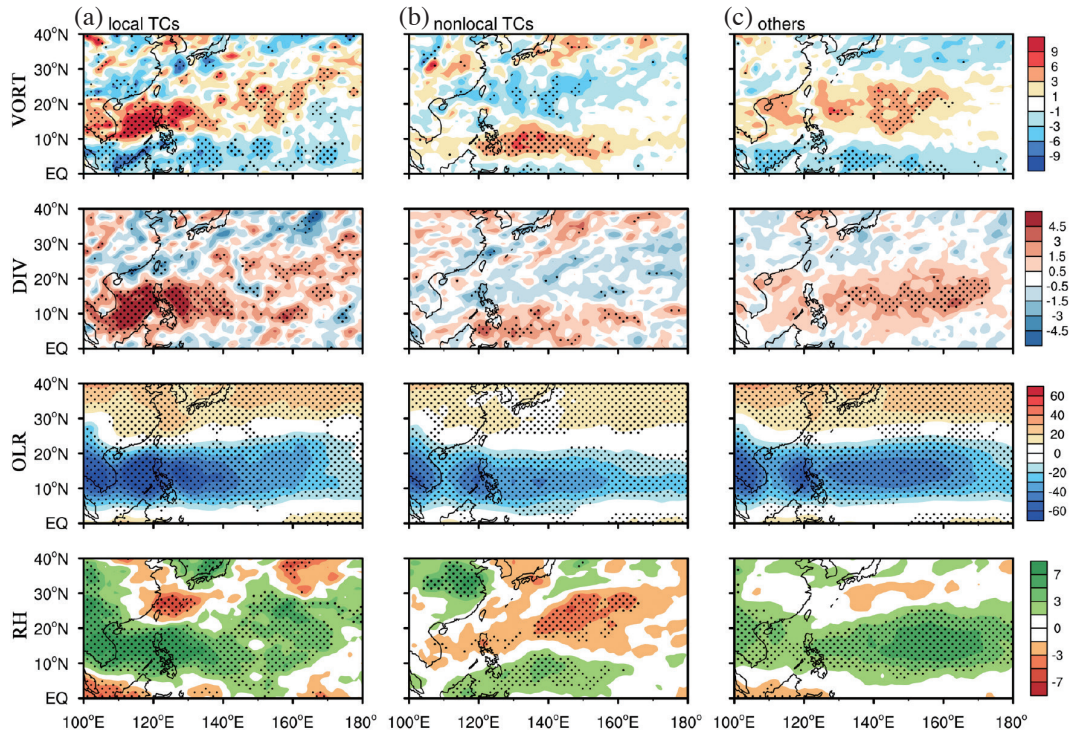


Fig. 4. The anomalous mean 850-hPa relative vorticity (Vort, 10^{-6} s^{-1}), 200-hPa divergence (Div, 10^{-6} s^{-1}), OLR (m s^{-1}), and 500 - 700-hPa relative humidity (RH, %, middle panels) for average of 1 day prior to the genesis of (a) local TCs, (b) nonlocal TCs, and (c) other TCs. The dotted regions indicate areas exceeding a 95% confidence level using a Student t test.

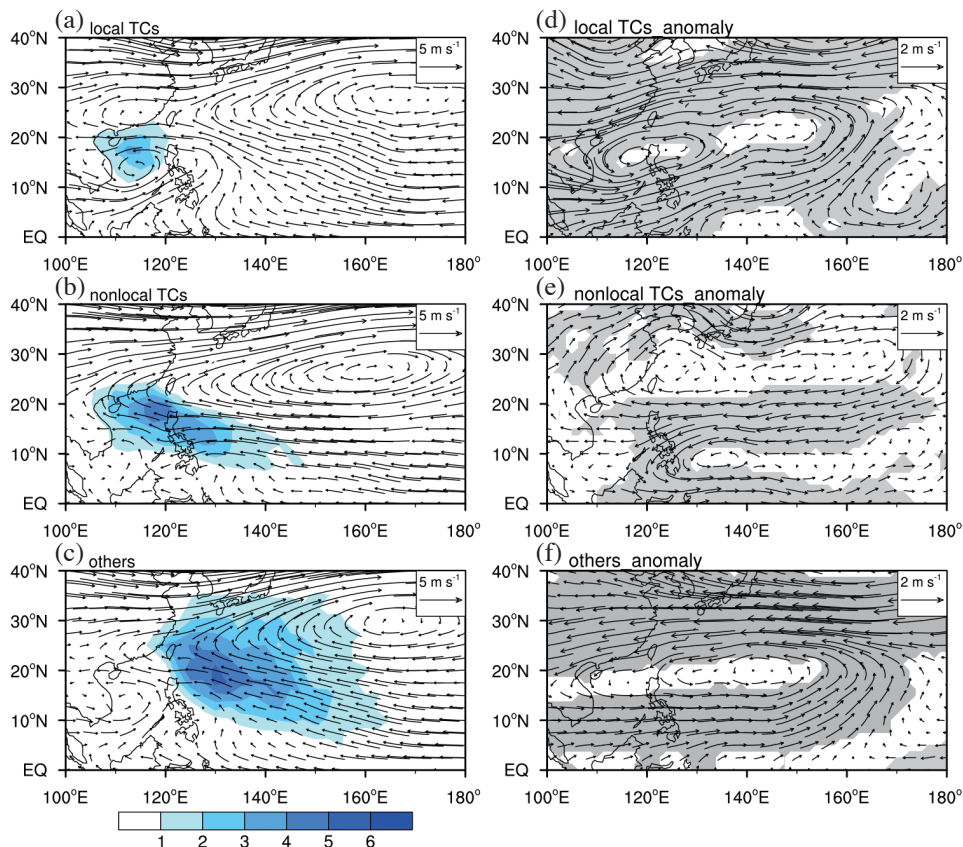


Fig. 5. As in Fig. 3, but for the TC occurrences (in a $2.5^\circ \times 2.5^\circ$ box, shaded) and large-scale steering flows (m s^{-1} ; vector). The large-scale steering flow can be defined as the mean flow from 850 to 300 hPa.

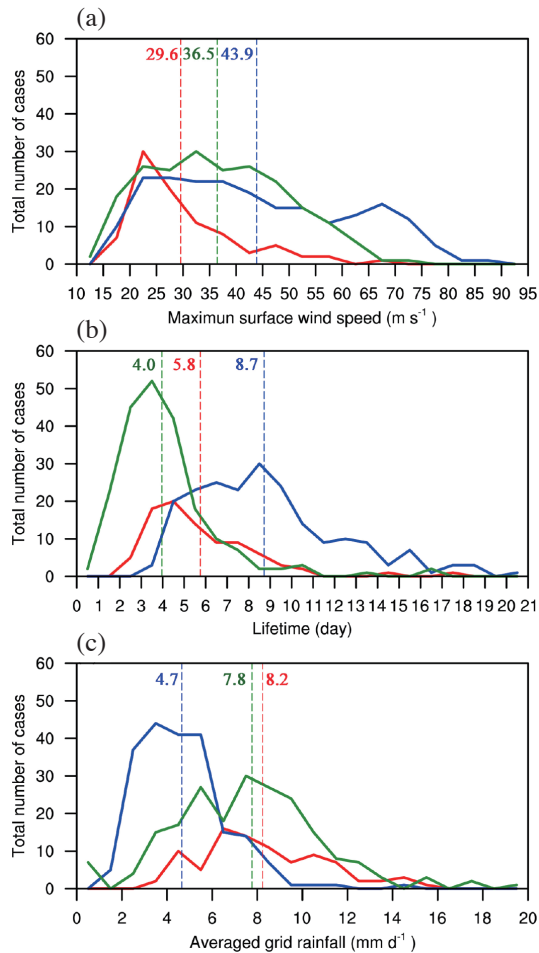


Fig. 6. Histograms of (a) maximum wind speeds (m s^{-1} ; one value per storm), (b) lifetime (day), and (c) averaged grid rainfall (mm h^{-1}) for each SCS basin storm for 1979 - 2016 (June to November). Individual curves are for TC number with formation (blue line) within and passage (red line) into the South China Sea. The red and blue dashed lines represent averages for local and nonlocal TCs, respectively. The green lines are for number of nonlocal TCs using only the data in the SCS.

nonlocal TCs (Fig. 3b). Previous studies have shown that the intensities, lifetimes, and formation locations of TCs are closely related (Wang and Chan 2002; Camargo and Sobel 2005; Camargo et al. 2007; Wu et al. 2012). Figure 6b shows the lifetime distributions of local and nonlocal TCs. TCs show a significant shift toward shorter lifetimes (approximately 5.8 days) when they are generated in the SCS (local TCs). This tendency toward shorter lifetimes, which provide less time for the TCs to intensify, could explain the weaker intensity of local TCs. Nonlocal TCs have longer lifetimes (approximately 8.7 days), which lead to more intense TCs. To examine how sensitive the nonlocal TC characteristics to analysis region, additional calculation with use of only the data in the SCS was performed (Fig. 6). The result shows that their intensity become weaker when nonlocal TCs move to the SCS, but still greater than local TCs.

TCs often cause heavy rainfall. Figures 7a - f show

the mean spatial distribution of annual TC-induced rainfall and its contribution to total rainfall. The SCS TCs show the highest rainfall west of the Philippines with values exceeding 500 mm yr^{-1} , accounting for 30 - 57% of the mean annual rainfall in the SCS (Figs. 7a, d). The spatial patterns of local and nonlocal TC rainfall closely match the TC tracks (Figs. 5a, b). Maximum local TC rainfall is centered around the north SCS. Nonlocal TC rainfall is observed along TC tracks across the WNP and the SCS, with a pronounced maximum around the Philippines. Although annual TC rainfall in the SCS is primarily attributed to nonlocal TCs (Figs. 7e, f), the individual TC-induced rainfall of local TCs is higher than that of nonlocal TCs (Figs. 7g, h). The intensity of local TC rainfall is approximately 2 times that of nonlocal TCs (Fig. 6c). It is interesting to note that weak local TCs lead to more rainfall; it is therefore likely that TC rainfall is not tied to TC intensity. Figure 8a shows the rainfall of local and nonlocal TCs plotted against TC intensity (maximum wind speeds). TC rainfall and intensity exhibit a weak linear relationship for both the local and nonlocal TCs with deviations in the regression coefficients of 0.08 and 0.09, respectively. Enhanced TC intensity has no proportional effect on TC rainfall; however, both local and nonlocal TC rainfall clearly show linear (inversely proportional) responses to translation speed, indicating that TC rainfall in the SCS is associated with translation speeds such that a decrease in TC translation speed would enhance the intensity of rainfall of both local and nonlocal TCs. Local TCs exhibit slower translation speeds than nonlocal TCs, which leads to increases in TC rain rates. Therefore, when nonlocal TCs move to the SCS, although their intensity become weaker, their rain rates would increase as a result of slowdown of TC translation speed and the forced nature of the local environments such as the moisture transport and the topography (Fig. 6c). The rain rates (lifetimes) of nonlocal TCs in the SCS are still slightly fewer (remarkably shorter) than that of local TCs and result in less rainfall in the SCS region for each nonlocal TC (Figs. 7g, h).

4. INTERDECADAL RELATIONSHIP BETWEEN LOCAL AND NONLOCAL TCS

There are very significant interannual and interdecadal variations in the annual numbers both local and nonlocal TCs in the SCS (Fig. 9). These are decomposed into an interdecadal variation (running 5-year mean) and an interannual variation (deviation from running 5-year mean). Note that there is an apparent inverse relationship between the numbers of local and nonlocal TCs. The correlation coefficient of this relationship is -0.59 (-0.45) on an interdecadal (interannual) timescale at the 99% confidence level. Previous studies (Zuki and Lupo 2008; Goh and Chan 2009) have demonstrated that TC activity in the SCS is modulated by ENSO. However, our results show that the number of TCs is

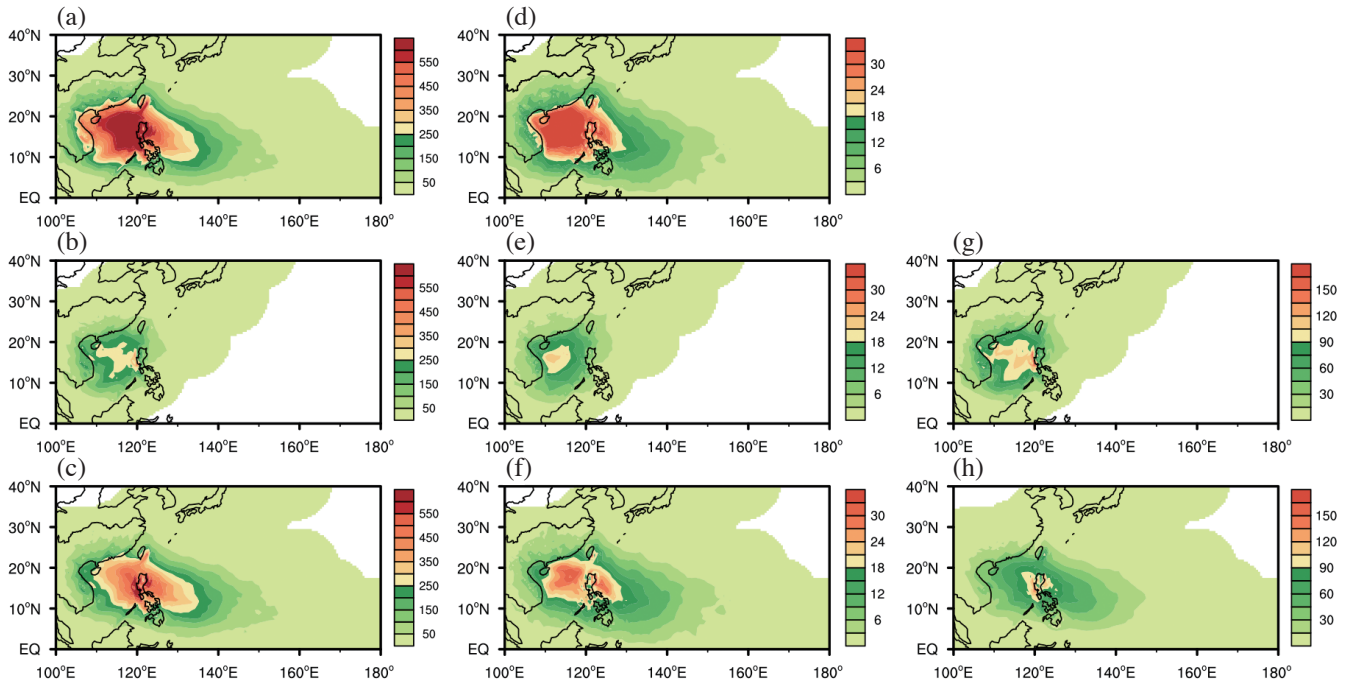


Fig. 7. Mean spatial distribution of (a) - (c) annual TC rainfall (mm), (d) - (f) relative contribution of TCs to total rainfall (%), and (g) - (h) each TC induced rainfall (mm) during June to November for (a) (d) all, (b) (e) (g) local, and (c) (f) (h) nonlocal TC in the SCS.

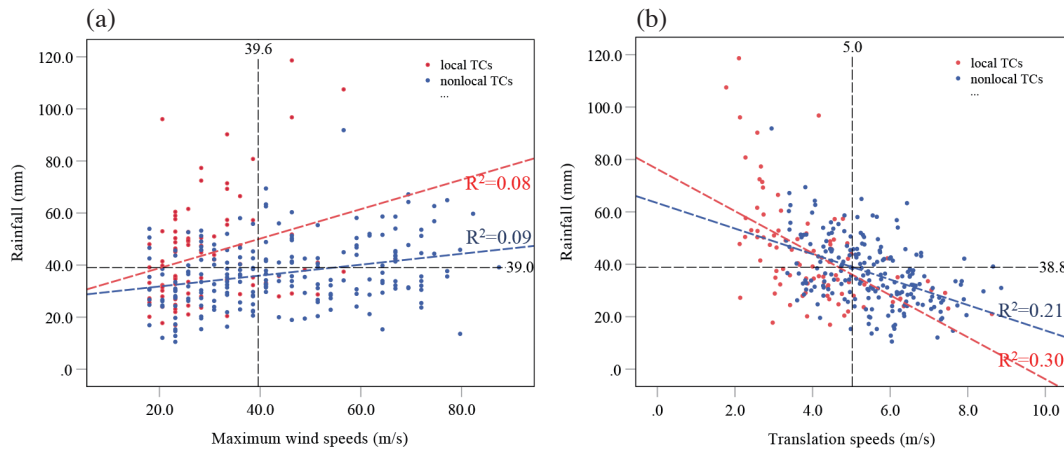


Fig. 8. Scatterplot of (a) maximum wind speeds and (b) translation speeds against rainfall of TCs. The red and blue colors correspond to local and nonlocal TC events, respectively. The dashed lines are the linear regressions, with the deviation of regression coefficients denoted by R^2 .

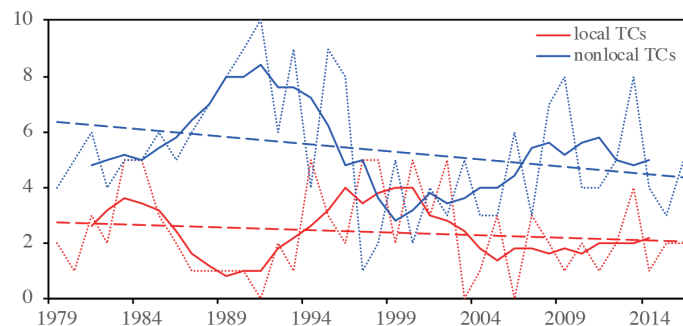


Fig. 9. Running 5-year mean (solid lines) and annual (dotted lines) genesis frequency of local TCs (red) and nonlocal TCs (blue) in the SCS during June to November for the period from 1979 through 2016. Least squares best-fit linear trends are depicted by the dashed lines.

weakly correlated with SST in the tropical Pacific, which is inconsistent with the earlier study of Zuki and Lupo (2008). This discrepancy is largely due to there being a slight and inconsistent difference in the numbers of TCs between the different ENSO phases (Table 1), which is similar to the results of Goh and Chan (2009) for the total number of SCS TCs.

The present study focuses on interdecadal variations. Note that there is an apparent inverse interdecadal relationship between the numbers of local and nonlocal TCs. Such a relationship can be explained by the atmospheric circulation anomaly associated with SST forcing. Previous studies have shown that the large-scale environmental conditions associated with SST forcing might be key to determining the variability of TC genesis. Figure 10 shows independent correlation charts of the June to November SST with the running 5-year mean numbers of local TCs and nonlocal TCs. The number of TCs is negatively correlated with the SST in the tropical central Pacific (155°E - 170°W; 0 - 10°N). For nonlocal TCs, such correlations are not only positively related to the SST in the tropical central and eastern Pacific, it is also negatively correlated with the SST in the extratropics and WNP, resembling the SST mode known as the Pacific Decadal Oscillation (PDO) pattern. Although their correlation patterns show distinct characteristics, the numbers of both local and nonlocal TCs exhibit strong linear responses to the SST of the tropical central Pacific. This suggests that the inverse relationship is a result of central Pacific SST forcing.

Figure 11 shows regressed charts of 850-hPa winds and TC genesis onto the time series of the 5-yr running mean of the SST in the tropical central Pacific (155°E - 170°W; 0 - 10°N). This enhanced SST heating in the central Pacific induces significant anomalous low-level westerlies centered over a region at 7.5°N between 130°E and 180° with anomalous cyclonic circulation in the north of the tropical WNP as a Gill-type Rossby wave response. Previous studies (Wu et al. 2012, 2018) suggested that these responses lead to weaker subtropical highs and enhanced westerly monsoonal winds, causing an enhanced MT to be shifted eastward and slightly northward. As a result, large-scale environmental conditions (such as stronger low-level cyclonic vorticity, upper-level divergence, and more mid-level relative humidity) associated with the eastern extension of the MT are favorable for enhanced TC genesis in the east of the Philippines and suppressed TC genesis in the SCS. While anomalous SST cooling in the central Pacific, it is vice versa.

5. SUMMARY

This study investigates the characteristics of TC activity over the SCS from June to November for the period of 1979 - 2016. There are two kinds of TCs in the SCS: those locally formed in the SCS (local TCs) and those travers-

ing the SCS (nonlocal TCs). The frequency of formation of nonlocal TCs is approximately 2 times that of local TCs. Nonlocal TCs tend to form in the WNP west of 160°E and cross the Philippines into the SCS with typical straight westward tracks. Local TCs mostly move northwestward or northeastward, and they have shorter tracks, are less intense, and have shorter lifetimes compared to nonlocal TCs. Annual TC rainfall in the SCS is primarily attributed to nonlocal TCs, but the slower motion of local TCs (with weak intensity) increases TC rain-rate and intensity of extreme rainfall. Further analysis shows that the SCS monsoon gyre creates a favorable environment for local TC genesis and tracks. Following the westward extension of the enhanced subtropical high, an eastward extending monsoon trough and anomalous easterlies in its northern periphery (between 10 and 20°N) may be important contributors to the genesis and westward tracks of nonlocal TCs. Although the location of the monsoon trough does not show significant longitudinal variation with passage (nonlocal TCs) or without passage (others) into the SCS, a northeastward retreating and weaker subtropical high leads to a slightly northeastward shift of the monsoon trough and of TC genesis compared to nonlocal TCs. Anomalous easterlies of the steering flows north of 20°N, as part of the retreating subtropical high, can be mostly contributed to northwestward and recurve tracks of other TCs in the WNP.

The annual numbers of local and nonlocal TCs exhibit an apparent inverse relationship. This inverse relationship appears on both interannual and interdecadal timescales, but is predominantly interdecadal. Although the SST patterns associated with local and nonlocal TCs show distinct characteristics, the central Pacific, which is an overlapping region of the significant correlations, may be a key region to this inverse relationship. The interdecadal variability of SST in the central Pacific leads to anomalous cyclonic activity over a farther northwest region, with significantly increased anomalous westerlies centered at 7.5°N because of a Gill-type Rossby wave response, and thus an enhanced eastward extension of the monsoon trough. Accompanied with these changes in the location and intensity of the monsoon trough, the primary environmental conditions are favorable for enhanced TC genesis in the east of the Philippines and for suppressed TC genesis in the SCS. This is an important reason for the inverse linkage between local and nonlocal TCs over the SCS.

These findings are important for fully understanding TC activity over the SCS. However, this study focused mainly on the climatologic characteristics of local and nonlocal TCs and their possible causes. Further investigation into the mechanisms of several different aspects of local and nonlocal TCs is needed.

Acknowledgements This work is jointly supported by the National Natural Science Foundation of China Grant 41875117, 41475077, and 41775056, and the Youth

Table 1. Average number of local and nonlocal TCs for El Niño, El Niño Modoki, La Niña, and all years.

	Local TCs	Nonlocal TCs
El Niño	2.2	4.6*
El Niño Modoki	1.8*	6.0
La Niña	2.7	5.0*
All years	2.3	5.5

Note: The asterisks indicate that the statistically significant at the 95% level.

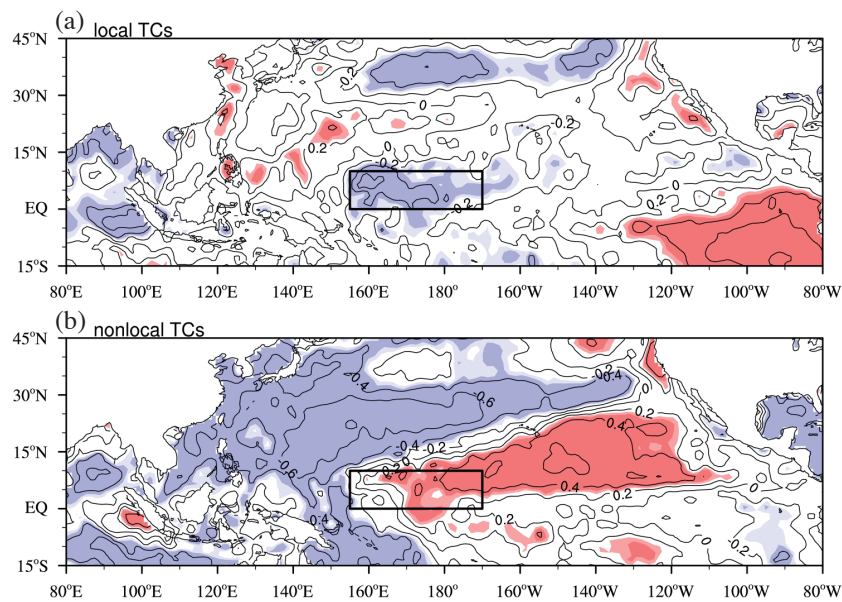


Fig. 10. Spatial distribution of correlation of June to November SST anomalies with running 5-year mean of the numbers of (a) local TCs and (b) nonlocal TCs. Significant values at 95% confidence level are shown in dotted regions.

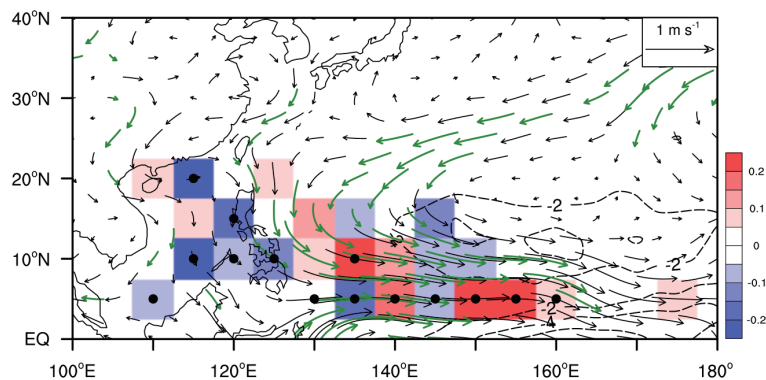


Fig. 11. Regression of 850 hPa wind anomalies (m s^{-1} , vector; significant values at 95% confidence level are shown in green arrows), OLR anomalies (W m^{-2} , contours shown are -2, -4, and -6), and TC genesis anomalies (shading) during June to November upon the tropical SST index (defined as running 5-year mean of June to November averaged over 108 - 120°E, 5 - 22°N).

Innovation Promotion Association CAS 2017106. Dr. Jau-Ming Chen was supported by Minister of Science and Technology, Taiwan, under grant MOST 106-2111-M-022-001-MY2.

REFERENCES

- Ashok, K., S. K. Behera, S. A. Rao, H. Weng, and T. Yamagata, 2007: El Niño Modoki and its possible teleconnection. *J. Geophys. Res.*, **112**, C11007, doi: 10.1029/2006JC003798. [[Link](#)]
- Bagtasa, G., 2017: Contribution of Tropical Cyclones to Rainfall in the Philippines. *J. Clim.*, **30**, 3621-3633, doi: 10.1175/JCLI-D-16-0150.1. [[Link](#)]
- Briegel, L. M. and W. M. Frank, 1997: Large-Scale Influences on Tropical Cyclogenesis in the Western North Pacific. *Mon. Weather Rev.*, **125**, 1397-1413, doi: 10.1175/1520-0493(1997)125<1397:lsiotc>2.0.co;2. [[Link](#)]
- Camargo, S. J. and A. H. Sobel, 2005: Western North Pacific tropical cyclone intensity and ENSO. *J. Clim.*, **18**, 2996-3006, doi: 10.1175/JCLI3457.1. [[Link](#)]
- Camargo, S. J., K. A. Emanuel, and A. H. Sobel, 2007: Use of a genesis potential index to diagnose ENSO effects on tropical cyclone genesis. *J. Clim.*, **20**, 4819-4834, doi: 10.1175/JCLI4282.1. [[Link](#)]
- Chan, J. C. L. and K. S. Liu, 2004: Global warming and western North Pacific typhoon activity from an observational perspective. *J. Clim.*, **17**, 4590-4602, doi: 10.1175/3240.1. [[Link](#)]
- Chen, J.-M., P.-H. Tan, L. Wu, J.-S. Liu, and H.-S. Chen, 2017: Climatological analysis of passage-type tropical cyclones from the Western North Pacific into the South China Sea. *Terr. Atmos. Ocean. Sci.*, **28**, 327-343, doi: 10.3319/TAO.2016.10.04.02. [[Link](#)]
- Cheung, K. K. W., 2004: Large-Scale Environmental Parameters Associated with Tropical Cyclone Formations in the Western North Pacific. *J. Clim.*, **17**, 466-484, doi: 10.1175/1520-0442(2004)017<0466:lepawt>2.0.co;2. [[Link](#)]
- Chu, P.-S., 2002: Large-scale circulation features associated with decadal variations of tropical cyclone activity over the central North Pacific. *J. Clim.*, **15**, 2678-2689, doi: 10.1175/1520-0442(2002)015<2678:lscfaw>2.0.co;2. [[Link](#)]
- Goh, A. Z.-C. and J. C. L. Chan, 2009: Interannual and interdecadal variations of tropical cyclone activity in the South China Sea. *Int. J. Climatol.*, **30**, 827-843, doi: 10.1002/joc.1943. [[Link](#)]
- Gray, W. M., 1968: Global view of the origin of tropical disturbances and storms. *Mon. Weather Rev.*, **96**, 669-700, doi: 10.1175/1520-0493(1968)096<0669:gvotoo>2.0.co;2. [[Link](#)]
- Gray, W. M., 1975: Tropical Cyclone Genesis, Atmospheric Science Paper No. 234, Department of Atmospheric Science, Colorado State University, Fort Collins, Colorado, 121 pp.
- Holland, G. J., 1983: Tropical cyclone motion: Environmental interaction plus a beta effect. *J. Atmos. Sci.*, **40**, 328-342, doi: 10.1175/1520-0469(1983)040<0328:tc-meip>2.0.co;2. [[Link](#)]
- Kobayashi, S., Y. Ota, Y. Harada, A. Ebata, M. Moriya, H. Onoda, K. Onogi, H. Kamahori, C. Kobayashi, H. Endo, K. Miyaoka, and K. Takahashi, 2015: The JRA-55 Reanalysis: General Specifications and Basic Characteristics. *J. Meteorol. Soc. Jpn.*, **93**, 5-48, doi: 10.2151/jmsj.2015-001. [[Link](#)]
- Kubota, H. and B. Wang, 2009: How Much Do Tropical Cyclones Affect Seasonal and Interannual Rainfall Variability over the Western North Pacific? *J. Clim.*, **22**, 5495-5510, doi: 10.1175/2009JCLI2646.1. [[Link](#)]
- Liebmann, B. and C. A. Smith, 1996: Description of a Complete (Interpolated) Outgoing Longwave Radiation Dataset. *Bull. Amer. Meteorol. Soc.*, **77**, 1275-1277.
- Ling, Z., Y. Wang, and G. Wang, 2016: Impact of Intra-seasonal Oscillations on the Activity of Tropical Cyclones in Summer over the South China Sea. Part I: Local Tropical Cyclones. *J. Clim.*, **29**, 855-868, doi: 10.1175/JCLI-D-15-0617.1. [[Link](#)]
- Ramsay, H. A., L. M. Leslie, P. J. Lamb, M. B. Richman, and M. Leplastrier, 2008: Interannual Variability of Tropical Cyclones in the Australian Region: Role of Large-Scale Environment. *J. Clim.*, **21**, 1083-1103, doi: 10.1175/2007JCLI1970.1. [[Link](#)]
- Rayner, N. A., D. E. Parker, E. B. Horton, C. K. Folland, L. V. Alexander, D. P. Rowell, E. C. Kent, and A. Kaplan, 2003: Global analyses of sea surface temperature, sea ice, and night marine air temperature since the late nineteenth century. *J. Geophys. Res.*, **108**, doi: 10.1029/2002JD002670. [[Link](#)]
- Saha, S., S. Moorthi, H.-L. Pan, X. Wu, J. Wang, S. Nadiga, P. Tripp, R. Kistler, J. Woollen, D. Behringer, H. Liu, D. Stokes, R. Grumbine, G. Gayno, J. Wang, Y.-T. Hou, H. Chuang, H.-M. H. Juang, J. Sela, M. Iredell, R. Treadon, D. Kleist, P. Van Delst, D. Keyser, J. Derber, M. Ek, J. Meng, H. Wei, R. Yang, S. Lord, H. van den Dool, A. Kumar, W. Wang, C. Long, M. Chelliah, Y. Xue, B. Huang, J.-K. Schemm, W. Ebisuzaki, R. Lin, P. Xie, M. Chen, S. Zhou, W. Higgins, C.-Z. Zou, Q. Liu, Y. Chen, Y. Han, L. Cucurull, R. W. Reynolds, G. Rutledge, and M. Goldberg, 2010: The NCEP Climate Forecast System Reanalysis. *Bull. Amer. Meteorol. Soc.*, **91**, 1015-1058, doi: 10.1175/2010BAMS3001.1. [[Link](#)]
- Simpson, R. H. and H. Riehl, 1981: The Hurricane and Its Impact, Louisiana State University Press, 398 pp.
- Sobel, A. H. and S. J. Camargo, 2005: Influence of western

- North Pacific tropical cyclones on their large-scale environment. *J. Atmos. Sci.*, **62**, 3396-3407, doi: 10.1175/jas3539.1. [[Link](#)]
- Wang, B. and J. C. L. Chan, 2002: How Strong ENSO Events Affect Tropical Storm Activity over the Western North Pacific. *J. Clim.*, **15**, 1643-1658, doi: 10.1175/1520-0442(2002)015<1643:hseeat>2.0.co;2. [[Link](#)]
- Wang, B., B. Xiang, and J.-Y. Lee, 2013: Subtropical High predictability establishes a promising way for monsoon and tropical storm predictions. *Proc. Natl. Acad. Sci.*, **110**, 2718-2722, doi: 10.1073/pnas.1214626110. [[Link](#)]
- Wu, L. and B. Wang, 2004: Assessing Impacts of Global Warming on Tropical Cyclone Tracks. *J. Clim.*, **17**, 1686-1698, doi: 10.1175/1520-0442(2004)017<1686:aiogwo>2.0.co;2. [[Link](#)]
- Wu, L. and H. Zhao, 2012: Dynamically Derived Tropical Cyclone Intensity Changes over the Western North Pacific. *J. Clim.*, **25**, 89-98, doi: 10.1175/2011JCLI4139.1. [[Link](#)]
- Wu, L., Z. Wen, R. Huang, and R. Wu, 2012: Possible Linkage between the Monsoon Trough Variability and the Tropical Cyclone Activity over the Western North Pacific. *Mon. Weather Rev.*, **140**, 140-150, doi: 10.1175/mwr-d-11-00078.1. [[Link](#)]
- Wu, L., H. Zhang, J.-M. Chen, and T. Feng, 2018: Impact of Two Types of El Niño on Tropical Cyclones over the Western North Pacific: Sensitivity to Location and Intensity of Pacific Warming. *J. Clim.*, **31**, 1725-1742, doi: 10.1175/JCLI-D-17-0298.1. [[Link](#)]
- Wu, P. and P.-S. Chu, 2007: Characteristics of tropical cyclone activity over the eastern North Pacific: The extremely active 1992 and the inactive 1977. *Tellus*, **59A**, 444-454, doi: 10.1111/j.1600-0870.2007.00248.x. [[Link](#)]
- Yang, L., Y. Du, D. Wang, C. Wang, and X. Wang, 2015: Impact of intraseasonal oscillation on the tropical cyclone track in the South China Sea. *Climate Dyn.*, **44**, 1505-1519, doi: 10.1007/s00382-014-2180-y. [[Link](#)]
- Zuki, Z. M. and A. R. Lupo, 2008: Interannual variability of tropical cyclone activity in the southern South China Sea. *J. Geophys. Res.*, **113**, D06106, doi: 10.1029/2007JD009218. [[Link](#)]